Science Bulletin 64 (2019) 941–952

Contents lists available at ScienceDirect

Science Bulletin

journal homepage: www.elsevier.com/locate/scib

Article

Mitigating self-excited flame pulsating and thermoacoustic oscillations using perforated liners

Dan Zhao [a,*], Ephraim Gutmark [b], Arne Reinecke [c]

[a] Department of Mechanical Engineering, College of Engineering, University of Canterbury, Christchurch 8140, New Zealand
[b] Department of Aerospace Engineering and Engineering Mechanics, University of Cincinnati, Cincinnati, OH 45221-0070, USA
[c] School of Mechanical and Aerospace Engineering, Nanyang Technological University, Singapore 639798, Singapore

ARTICLE INFO

Article history:
Received 28 February 2019
Received in revised form 5 April 2019
Accepted 9 May 2019
Available online 15 May 2019

Keywords:
Flame beating
Combustion instability
Thermo-acoustic instability
Thermal-diffusive instability
Perforated pipe
Acoustic losses

ABSTRACT

Open-loop control of self-excited flame pulsating oscillations and thermo-acoustic instability is considered in this work. The performance of the control strategy is numerically evaluated in a 2D Rijke-type combustor with a perforated pipe implemented. It is found that approximately 38 dB sound pressure level (SPL) reduction can be achieved by actively tuning the cooling flow through the perforated pipe. Furthermore, the vorticity-induced damping performance is contributing to the breaking up of flame-acoustics coupling. However, the shedding of vortices is not uniformly distributed along the perforated pipe. To apply the control strategy in practice and to validate the findings, experimental studies are performed on a customer-designed Rijke-type combustor with a perforated liner implemented. To mimic practical engines, a cooling flow generated by a centrifugal pump is provided to pass through the perforated pipe. Properly tuning the cooling flow rate is found to lead to the unstable combustor being successfully stabilized. SPL is reduced by approximately 35 dB at $\omega_1/2\pi \approx 245$ Hz, and harmonic thermoacoustic modes are completely attenuating. Further study is conducted by suddenly removing the perforated pipe section. The combustion system is found to be associated with not only classical thermo-acoustic limit cycle oscillations with a dominant mode at 2.45×10^2 Hz, but also beating oscillations at 1.4×10^0 Hz. It is revealed that increasing acoustic losses by implementing the perforated pipe is another critical mechanism contributing to attenuating flame pulsating instability. The present work opens up an applicable means to attenuate both self-excited high-frequency thermoacoustic and low-frequency flame pulsating oscillations.

1. Introduction

Self-sustained nonlinear thermoacoustic oscillations are desirable in some applications, for example refrigeration [1,2]. However, they are unwanted in gas turbines and aeroengines. The frequent occurrence of such detrimental thermoacoustic oscillations in lean, premixed combustors continues to hinder the development of modern gas turbine engines [3]. These oscillations in the combustors are generally generated due to the dynamic interactions between oscillatory flow and unsteady heat release processes [4]. These instabilities characterized by large-amplitude periodic oscillations are undesirable, since they can significantly decrease the lifetime and regions of safe operability of the combustors [5]. Although extensive efforts have been made, how to effectively control flame pulsation (also known as beating oscillations) and thermo-acoustic instabilities in modern aeroengines and land-based gas turbines remains a challenge at the design stage. In these unwanted flame pulsating and/or thermo-acoustic oscillation regimes, a dynamic and nonlinear flame-acoustic coupling occurs [6,7]. These oscillations can lead to structural vibration and overheating, even harmful consequences. Thus understanding the occurrence and growth of these thermo-acoustic and flame pulsating modes requires knowledge not only of the flame dynamics but also the effects of the acoustic conditions on the stability of the combustor.

Some thermo-acoustic combustors are found to be associated with time-variant pressure amplitudes. Lieuwen [5] experimentally studied limit cycle oscillations in an unstable premixed combustor. Here a bluff body was used to anchor the flame. It was found that small-amplitude beating oscillations occurs occasionally, shortly before the system evolved into large-amplitude limit cycles. However, no further investigations are conducted on the beating oscillations, such as the frequency, amplitude and flame motion characteristics. Chatterjee et al. [8] experimentally and numerically studied a closed-open unstable Rijke combustor in Virginia tech. A low-frequency mode characterizing flame

* Corresponding author.
E-mail address: dan.zhao@canterbury.ac.nz (D. Zhao).

https://doi.org/10.1016/j.scib.2019.05.004
2095-9273/

pulsating instability between 10 and 20 Hz was experimentally measured. According to Margolis [9], it is classified as a type of thermal-diffusive instability, which excites the flame-sheet to move toward and away from the burner periodically. Recently, Weng et al. [10–12] experimentally and numerically studied an unstable Rijke burner. As the equivalence ratio was set to the upper and lower limit, both beating oscillations and thermo-acoustic limit cycles at dramatically different time scales were co-existing. To simulate the experiments, a flame model incorporating both time scales was proposed. Flame heat loss is identified to play a critical role in low frequency flame pulsations. However, it would be interesting to know if there is any other losses such as acoustics or flow contributing to the low frequency flame pulsation.

Flame pulsating instability under acoustic excitation was experimentally observed at large Lewis numbers [13]. A thermo-acoustic field was generated in a tube to increase conductive and radiative heat loss, which enabled a clear observation of the pulsating motion. This is due to the fact that acoustic pressure suppressed the intrinsic hydrodynamic instability arising from thermal expansion. Mejia et al. [14] experimentally and numerically assessed the effect of flame-holder temperature on the flame transfer function (FTF) of a laminar flame. The formation of a recirculation zone is found to affect strongly on the FTF, when a cooled flame-holder is considered. Kabiraj and Sujith [15] experimentally studied nonlinear transition of thermo-acoustic instabilities to flame blowout via intermittency in a duct burner with a premixed flame. The flame was observed to undergo intermittent lift-off and reattachment. They argued that such motions arisen from the Kelvin-Helmholtz instability of the jet flow.

The flame dynamic responses to flow/acoustic disturbances have been extensively investigated [12]. Saurabh and Paschereit [16] experimentally studied the dynamic response of a swirl-stabilized premixed flame to transverse acoustic disturbances to gain insight on the occurrence and characteristics of thermo-acoustic instability in an annular combustor. It was found that transverse acoustic disturbance affected the responses of the flame quite differently in comparison acoustic forcing at low frequencies. Li et al. [17] numerically predicted the occurrence of thermo-acoustic instability, when a long flame was confined in a combustor. Blumenthal et al. [18] theoretically studied the linear response of premixed laminar flames to different types of velocity disturbances via impulse response functions. The flame responses consist of a convective motion and a restoring motion resulting from the combined effects of flame propagation and anchoring.

The effect of the acoustic boundaries [19] and boundary losses is barely known, as it is difficult to control in reacting flow configurations. However, for a few of simple and well-controlled configurations, predictive means [20] have already been developed. These means are generally applicable to the specific studied configuration. There is no universal modelling developed. Since there is a lack of prediction capacity, various approaches such as active or passive means [21–23] have been developed to attenuate the oscillations resulting from these instabilities. Active control can be implemented. There are two configurations: open- and closed-loop (feedback). Open-loop control of thermo-acoustic instability was experimentally tested by Cosic et al. [24] on an atmospheric combustor. Open-loop tuning of the acoustic and fuel flow forcing at different frequencies and intensities were applied to attenuate limit cycle oscillations. Uhm and Acharya [25,26] applied high-momentum air jet to open-loop active control of combustion instabilities in a swirl-stabilized spray combustor. The oscillation amplitude is found to be reduced by a factor of approximately 10. A more complete review of open-loop active control of combustion systems was conducted on a gas turbine engine by Richards et al. [27,28]. It is often used to control some input parameters, such as secondary fuel injection, or to modulate the acoustic conditions at inlet or outlet of the combustor [29]. Compared with closed-loop configurations, open-loop approach has some attractive features such as no need of high-fidelity fuel actuators and easier implementation [30]. However, active control typically involves a complex and costly modification of the combustion chamber. It is intensively studied in academic communities but unapplicable in engine industries.

Passive control methods [31] are more reliable and robust and effective, when designed properly. Some solutions have already been proved to be applicable in real configurations [32,33]. The proper design of passive means involves optimal placement of acoustic dampers [34–37], such as quarter-wave resonators, Helmholtz resonators [34], or perforated liners [35]. They are generally used to dampen specific tonable noise. Perforated liners [36] are widely applied in mufflers. They have been the focus of many previous and on-going studies, due to their low cost and efficiency. Their damping capacities are improved, if they are backed by a resonant cavity [38]. Furthermore, to protect the liners and to promote the combustor wall cooling, a cooling flow is needed, which is known as bias flow [39]. As the bias flow through the perforated liners, the acoustic damping performance of the liners can be dramatically increased, due to the enhanced vortex shedding [40]. Nonlinear interactions between the cooling flow and the perforated liners may lead to high level of acoustic pressure fluctuations [41,42] due to incorrect implementation.

This paper describes the results of an experimental and numerical investigation of both flame pulsating and limit cycle thermo-acoustic oscillations in a Rijke-type combustor. Specially, it presents an open-loop active control approach that is effective for damping these 2 types of oscillations and identifying another mechanism contributing to attenuating low-frequency flame pulsating instability, besides the flame heat loss as identified in the previous work [10].

2. Numerical simulations

To evaluate the idea of open-loop active control of perforated pipe's damping on attenuating combustion instability, a lined Rijke-type combustor with a controllable cooling flow is numerically modelled as shown in Fig. 1. The total length L_{tot} of the combustor is $L_{tot} = 80$ cm. A premixed propane-fueled flame is confined at $L_f = 13$ cm away from the bottom inlet. A perforated pipe with a large back cavity is implemented at $L_f + L_d = 52$ cm downstream of the flame. The length and the inner diameter of the perforated pipe are $L_l = 10$ cm and $D = 45$ mm respectively. The boundary conditions are set as: the bottom open end is pressure inlet, while the top open end is pressure outlet. Note that the geometric dimensions and the boundary conditions of the modelled combustor are following closely those of the experimental setup as described in the following section.

Time-dependent 2D simulations are conducted by using the general purpose CFD code: ANSYS Fluent 15.0. Previous studies [44,43] have confirmed that Fluent is able to simulate the unsteady combustion-flow-acoustics interaction. It employs a control-volume based finite-difference method to solve the unsteady conservation equations of mass as

$$\frac{\partial \rho}{\partial t} + \frac{\partial (\rho u_i)}{\partial x_i} = 0, \tag{1}$$

where ρ is density, u is fluid velocity, t is time and x denotes the spacial dimension. The momentum conservation equation is

$$\frac{\partial (\rho u_i)}{\partial t} + \frac{\partial (\rho u_i u_j)}{\partial x_i} = -\frac{\partial p}{\partial x_i} + \frac{\partial}{\partial x_i}\left[\mu_t\left(\frac{\partial u_i}{\partial x_j} + \frac{\partial u_j}{\partial x_i}\right) - \frac{2}{3}\mu_t \frac{\partial u_k}{\partial x_k}\right]\delta_{ij}, \tag{2}$$

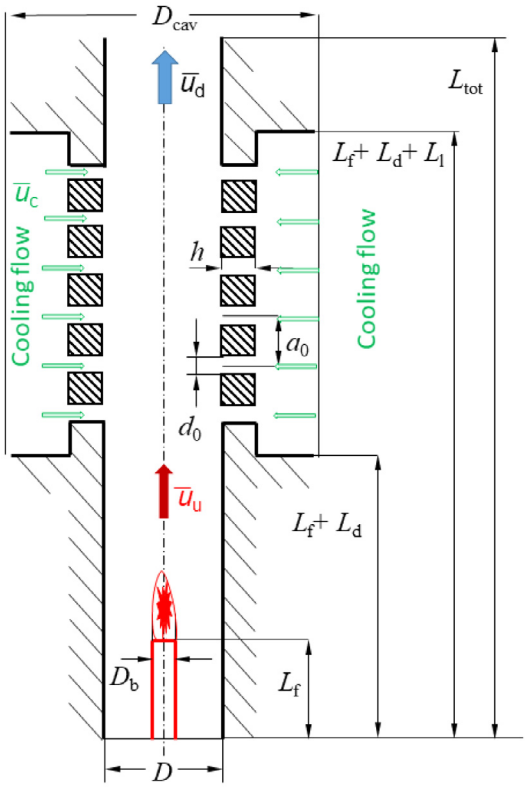

Fig. 1. (Color online) Geometry and dimension of the modelled Rijke-type combustor with a perforated pipe implemented. $D_b = 5$ mm, $a_0 = 10$ mm, $d_0 = 3$ mm, $D_{cav} = 200$ mm, and $h = 5$ mm.

where p is pressure, μ_t is turbulent viscosity, and δ_{ij} denotes Kronecker delta function. The conservation equation for the species fractions is

$$\frac{\partial(\rho\chi_k)}{\partial t}+\frac{\partial(\rho u_i\chi_k)}{\partial x_i}=-\frac{\partial J_k}{\partial x_i}+R_k, \tag{3}$$

where χ_k denotes the k^{th} species mass fraction, J_k is the diffusion of the species, and R_k is the production of the species due to chemical reaction.

The energy conservation equation is

$$\frac{\partial(\rho E)}{\partial t}+\frac{\partial[u_i(\rho E+p)]}{\partial x_i}=\frac{\partial}{\partial x_j}\left(k_{eff}\frac{\partial T}{\partial x_j}-\sum_j h_j J_j+u_i\left[\mu_{eff}\left(\frac{\partial u_j}{\partial x_i}+\frac{\partial u_i}{\partial x_j}\right)-\frac{2}{3}\mu_{eff}\frac{\partial u_k}{\partial x_k}\delta_{ij}\right]\right), \tag{4}$$

where E denotes the total energy, k_{eff} is effective thermal conductivity, h denotes enthalpy, μ_{eff} is effective viscosity, and T denotes the temperature.

In these conservation equations, the turbulent viscosity μ_t was introduced to model the effect of turbulence on the flow according to the Boussinesq hypothesis. This additional unknown needs to be determined via additional modeling, for which the RNG $k-\varepsilon$ model in Fluent is employed. The turbulent viscosity is computed from k, the turbulent kinetic energy, and ε, turbulent dissipation, as given in the following expression:

$$\mu_t=0.0845\rho\frac{k^2}{\varepsilon}. \tag{5}$$

Turbulent kinetic energy k and dissipation ε are determined from transport equations of similar structure to the governing equation for the fluid flow, as given as:

$$\frac{\partial(\rho k)}{\partial t}+\frac{\partial(\rho k u_i)}{\partial x_i}=\frac{\partial}{\partial x_j}\left(\alpha_k\mu_{eff}\frac{\partial k}{\partial x_j}\right)+G_k+G_b-\rho\varepsilon-Y_M, \tag{6}$$

and

$$\frac{\partial(\rho\varepsilon)}{\partial t}+\frac{\partial(\rho\varepsilon u_i)}{\partial x_i}=\frac{\partial}{\partial x_j}\left(\alpha_\varepsilon\mu_{eff}\frac{\partial\varepsilon}{\partial x_j}\right)+C_{1\varepsilon}\frac{\varepsilon}{k}(G_k+C_{3\varepsilon}G_b)-C_{2\varepsilon}\rho\frac{\varepsilon^2}{k}-R_\varepsilon, \tag{7}$$

where G_k and G_b denote the generation of turbulence kinetic energy due to mean velocity gradients and buoyancy. Y_M denotes the contribution of the fluctuating dilatation in compressible turbulence to the overall dissipation rate. The model constants are $C_{1\varepsilon} = 1.42, C_{12\varepsilon} = 1.68$. α_k and α_ε are inverse effective Prandtl number for k and ε respectively.

The combustion of propane in Fluent is simulated by a single-step reaction mechanism as given as

$$C_3H_8+5(O_2+3.76N_2)\longrightarrow 3CO_2+4H_2O+18.8N_2. \tag{8}$$

The eddy-dissipation model is used for determining the production term R_k in Eq. (3). This production term is computed according to the following expression:

$$R_k=\min\left(4.0\nu'_kM_k\rho\frac{\varepsilon}{k}\min_i\left(\frac{\chi_i}{\nu'_iM_i}\right),2.0\nu'_kM_k\rho\frac{\varepsilon}{k}\frac{\sum_i\chi_i}{\sum_j^N\nu''_jM_j}\right), \tag{9}$$

where ν' denotes the stoichiometric coefficient of reactants, M denotes the molecular weight of species.

Further details can be found in the relevant text book [45–47] or the Fluent documentation, which contains more information about the modeling of the governing equations. By solving these governing equations with the proper boundary conditions, the lined Rijke-type combustion system is numerically simulated. The essential properties of the CFD model are summarized here:

- pressure-based, coupled solver (Courant number 1.0), under-relaxation factors 0.90.
- unsteady simulation (time step size $\Delta t = 0.0001$ s, second order discretization).
- spatial discretization: second order pressure discretiation, third order MUSCL scheme.
- turbulence dissipation (second order upwind).
- fluid: ideal gas, propane-air mixture (air mass composition: nitrogen (76.8%), oxygen (23.2%))
- species transport model, volumetric reactions, eddy-dissipation turbulence-chemistry interaction
- boundary conditions:
  - tube and burner side walls – adiabatic
  - perforated pipe wall – adiabatic
  - burner tip – mass flow inlet
  - lower tube end – pressure inlet
  - upper tube end – pressure outlet
  - cavity side surface – adiabatic
  - cavity outer surface – mass flow inlet
  - cooling mass flow rate is tuned by applying a cosine-shaped function controlled via a UDF (user-defined function))
- turbulence model: $k-\varepsilon-RNG$
- gravitational acceleration $g = -9.81$ m/s^2 along the tube axial direction

It is worth noting that actively tuning of the cooling flow rate is achieved by Fluent's UDF (user defined function). The initial cooling mass flow rate is determined by evaluating the mass flow rate through the tube outlet, as no cooling flow is applied through the

perforated pipe. The boundary condition of the bias/cooling flow is set to be constant mass flow through the perforated liner. The cooling flow rate is then continuously varied by checking if the predicted pressure rms value is decreased.

The mesh consists exclusively of quadrilateral elements, in total 71,404 elements, from which 15,936 are located in the liner cavity and 54,428 in the open ended tube. There are 23 elements along bunsen burner outlet in radial direction and 53 elements for the remaining tube radius yielding 76 elements along tube radius. The tube has 348 elements along tube axial direction from inlet to liner section. The liner section is discretized with 332 elements in axial direction, followed by 64 elements for the remaining tube towards the outlet. Each of the 13 orifices is filled with 8 (in axial direction) times 10 elements (in radial direction). The liner cavity has 332 times 48 elements. The meshes near the regions of the liner section and the perforated orifices and the bunsen burner are illustrated in Fig. 2.

The model is validated first as discussed in the following section by comparing with our experimental measurements. It is then used to predict the performance of the bias-flow perforated liner on attenuating combustion oscillations as shown in Fig. 3. It can be seen from Fig. 3a that large-amplitude limit cycle oscillations are successfully produced, before the cooling flow is actuated at $t = 2.1$ s. However, as the cooling flow rate is increased at $t \geqslant 2.1$ s as shown in Fig. 3b, the combustion-driven pressure oscillations are attenuated. With the increased cooling flow rate, the limit cycle oscillations are completely attenuated at $t \approx 5.0$ s. Time evolution of the cooling flow rate is shown in Fig. 3c. For comparison, the inlet mass flow rate is also provided. It can be seen that minimizing the combustion-driven oscillations is achieved, when the mass flow ratio between the cooling and the inlet flow is approximately 205%.

Fig. 4 illustrates the phase diagrams of the unsteady heat release, as time is set to 4 different values. As the cooling flow rate is actively increased, $Q'(t)$ is decreased. And the phase diagram of the unsteady heat release $Q'(t)$ is changed from an elliptical-shape (see Fig. 4a) to a non-uniform shape as shown in Fig. 4d and shrink into a point. This indicates that there is negligible unsteady hear release and the flame front distortion should be minimized. This will be confirmed by checking the flame image as discuss later.

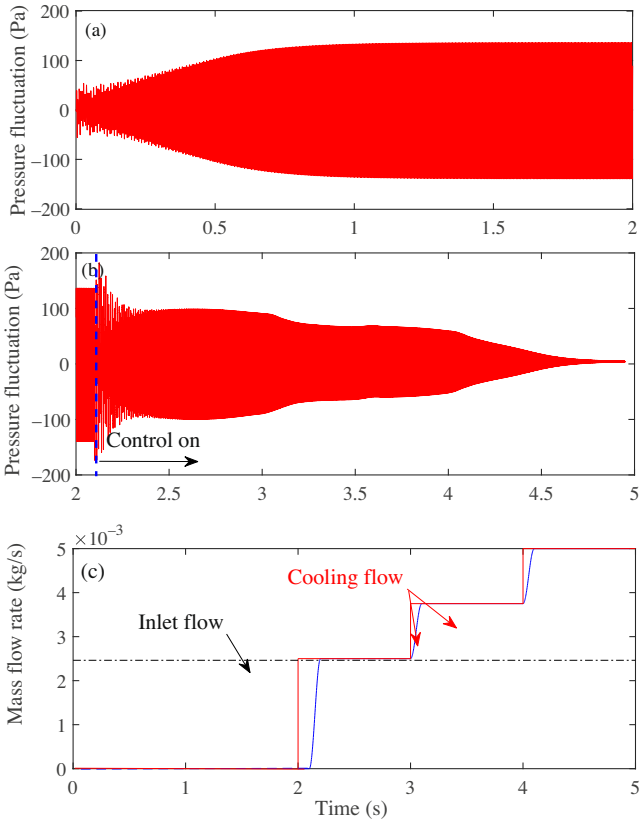

Fig. 3. (Color online) Time evolution of (a), (b) pressure fluctuation and (c) mass flow rate of the cooling flow and the combustor inlet flow.

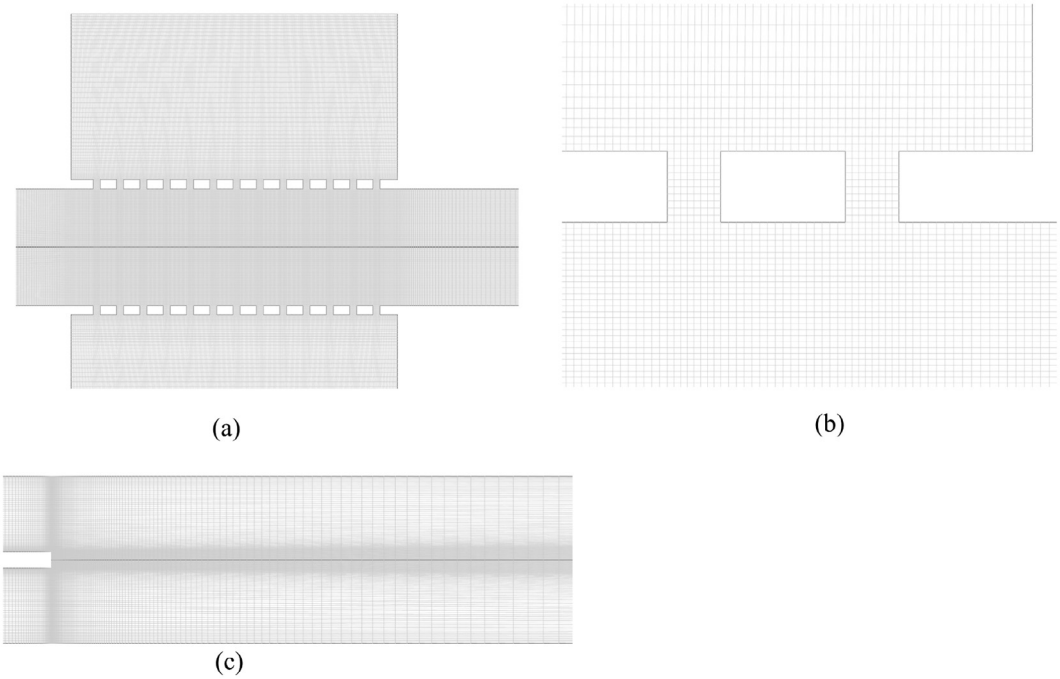

Fig. 2. Numerical meshes (a) in the lined cavity section, (b) zoom-in view of the mesh near the perforated orifices, (c) around the bunsen burner outlet.

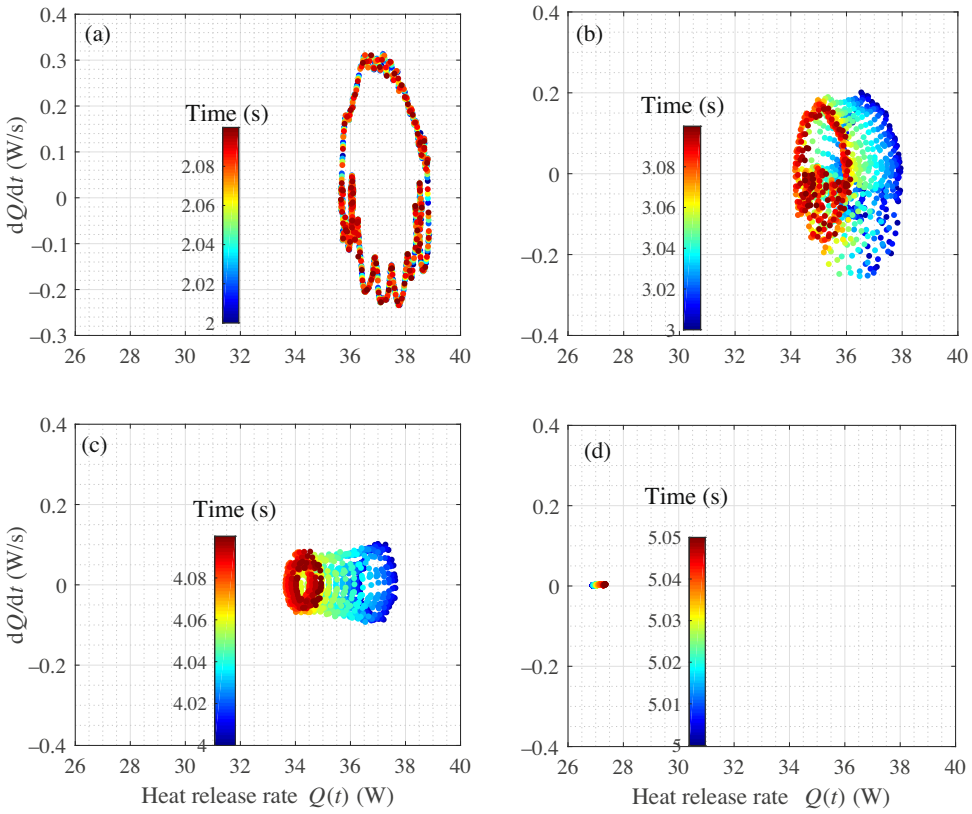

Fig. 4. (Color online) Phase diagrams of the unsteady heat release rate $Q(t)$ from the premixed flame, as time is set to 4 different values. (a) t = 2.0 s, (b) t = 3.0 s, (c) t = 4.0 s and (d) t = 5.0 s.

Fig. 5 shows the 2D contours of the heat of reaction and vorticity at the perforated pipe section. It can be seen from Fig. 5a and d that when no cooling flow is injected, limit cycle oscillations are produced. The flame front is in the wavy shapes and periodically varies in space and time. As the cooling flow rate is increased, combustion-driven oscillations are attenuated. The flame front is smoother and becomes smaller, as shown in Fig. 5b and c. This reveals that the flame shape distortion is mainly due to the acoustic disturbances. However, the vorticity generated through the perforated pipe is intensified, as shown in Fig. 5e and f. Furthermore, vorticity is not uniformly generated from the perforated pipe section along the axial direction. Further downstream, more intensified vortcity is produced. This is most likely due to the acoustics mode-shape along the tube axial direction. Near the pressure node, there is a larger pressure difference across the orifices and thus more vortices are produced.

3. Description of the experimental setup

To validate the numerical findings and to evaluate the potential of implementing the control strategy in practice, a lab-scale Rijke-type combustor is re-designed to incorporate a perforated pipe, which is enclosed by a large cavity (15 cm × 50 cm × 50 cm). To protect the perforated pipe, a cooling air flow, also known as a bias flow in the literature is applied. For this, a centrifugal pump is used to produce and force an ambient air flow through the perforated pipe with an orifice diameter of 3 mm and join the combustion flow in the Rijke tube as shown in Fig. 6a. A Bunsen burner with a premixed flame is used for the combustion experiment. The flame is confined in the lower half of a Rijke tube with a length of $L_f + L_d = 0.65$ m. It is placed at $L_f = 13$ cm from the bottom open end of the combustor.

The lined section is a cylindrical duct perforated with hundreds of tiny circle-shaped orifices. The length and diameter of the lined section are $L_l = 100$ mm and $D_l = D = 45$ mm. The perforated pipe is enclosed in the large cavity as shown in Fig. 6a. The geometry and dimension of the perforated pipe is summarized in Table 1.

A centrifugal pump is connected to the cavity to provide a cooling flow through the perforated pipe. The mass flow rate of the cooling flow is steady and controllable, by varying the voltage applied to the pump. In other words, constant mass flow rate of cooling air is supplied to the liner. A correlation between the pump voltage and the cooling flow velocity is provided in Supplementary materials. The voltage is tuned by monitoring the measured pressure rms value. For this, there is a pressure sensor located 400 mm away from the bottom open end of the Rijke tube. It is also a cylindrical duct. Its outer and inner diameters are 51 and 45 mm. When the lined section is removed, the setup is converted into a classical Rijke-type combustor with both ends acoustically open (see Fig. 6b). Since the experimental measured pressure rms values is used to monitor the stability condition/behaviours of the Rijke tube. If the rms value is too small, then the cooling flow rate is not increased any more (see Fig. 3c). This means that the measured pressure rms is a reference signal [48–51]. The cooling flow is an actuator. By following the previous classical review study [52], the current control approach is an open-loop active control.

4. Experimental results and discussion

4.1. Open-loop active control

Before the centrifugal pump is actuated (i.e. no cooling flow is injected through the perforate pipe), the flame-sustained combustion instability is successfully generated from the lined Rijke-type

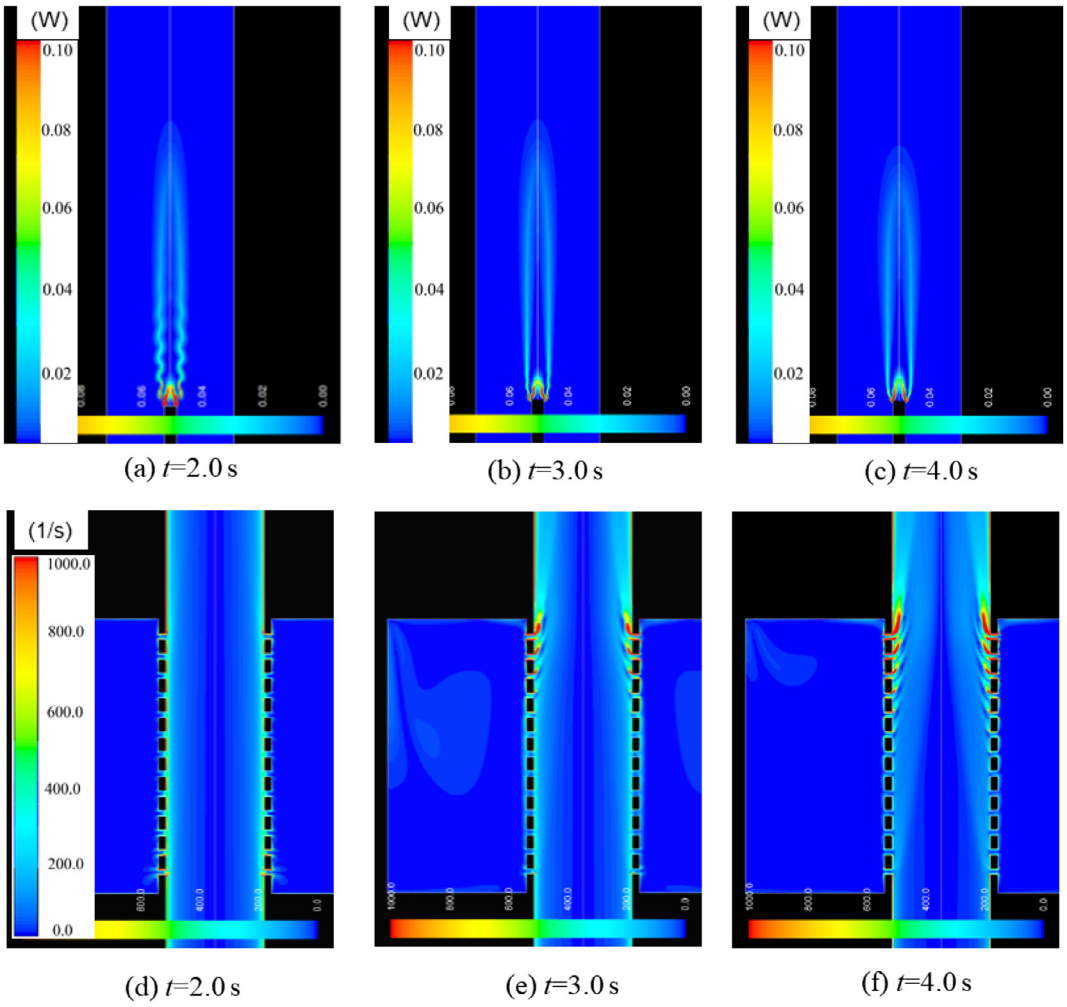

Fig. 5. (Color online) Two-dimensional contours of (a)–(c) heat of reaction from the premixed flame, (d)–(f) vorticity at the perforated pipe section, as time t is set to 3 different values.

combustor at $t \leqslant 18$ s, as shown in Fig. 7a. Here, the propane flow rate is 230 mL/s. However, as the pump is actuated at $t = 18$ s and actively control as shown in Fig. 7c, the combustion instability is attenuated somehow, depending on the cooling flow rate. The amplitude of the limit cycle is minimized at $t \geqslant 36$ s, as shown in Fig. 7b. However, as the pump is turned off at $t \geqslant 48$ s, the combustion-excited limit cycle oscillations are reproduced with almost the same amplitude. This reveals that the cooling flow rate plays an important role on attenuating combustion-excited oscillations.

Active control of the perforated pipe in the presence of a controllable cooling flow results in a sound pressure level (SPL) reduction of more than 35 dB at the fundamental frequency at $\omega_1/2\pi \approx 245$ Hz, as shown in Fig. 8a. Here the sound pressure level (SPL) with a unit of dB is defined as

$$\mathrm{SPL}(\omega) = 20\log_{10}\left(\frac{\|p'_{\mathrm{rms}}(\omega)\|}{p_{\mathrm{ref}}}\right), \tag{10}$$

where $\|p'_{\mathrm{rms}}(\omega)\|$ is the root mean square value of the pressure fluctuations. $p_{\mathrm{ref}} = 2.0 \times 10^{-5}$ Pa is the reference pressure.

The implementation of such active open-loop control strategy leads to the harmonics and sub-harmonics of combustion-excited oscillations being completely attenuated. The experimental results confirm that actively tuning the cooling flow rate through the perforated pipe can lead to unstable combustion system being successfully stabilized. Comparison between the experimental measurements and the numerical results are then made. It can be seen from Fig. 8a and b that the experimental and numerical results agree well in terms of SPL reduction and the dominant eigenmode at ω_1. Note that the experimental measurements are conducted by applying B&K microphones (type 4958). The microphones are calibrated by using a B&K 4228 pistonphone (124 dB@251 Hz). The unit of measurements is Pa. However, when we attempted to obtain frequency spectrum [53,54], we converted the amplitude of the pressure oscillation into dB by using the above definition of sound pressure level (SPL). Fig. 8c and d shows the comparison between the predicted and measured pressure fluctuations in time- and frequency-domain respectively [53]. It can be seen that a good agreement is obtained in terms of the amplitude and frequency of the oscillations. This confirms that the model is applicable to simulate the experiments. Finally, a closer observation of the dominant peak in the frequency spectrum (see Fig. 8d) reveals that there are some less apparent local peaks near the dominant one than what Weng et al. [11] found in their experiment. This is most likely due to the fact that an additional bias-flow perforated liner is attached to the Rijke-type combustor. In general, the observation of these frequencies are consistent with the previous observation in Weng et al.'s experiments.

4.2. Damping flame pulsating oscillations

Further study is then conducted on the lined Rijke-type combustor by suddenly but gently removing the perforated pipe sec-

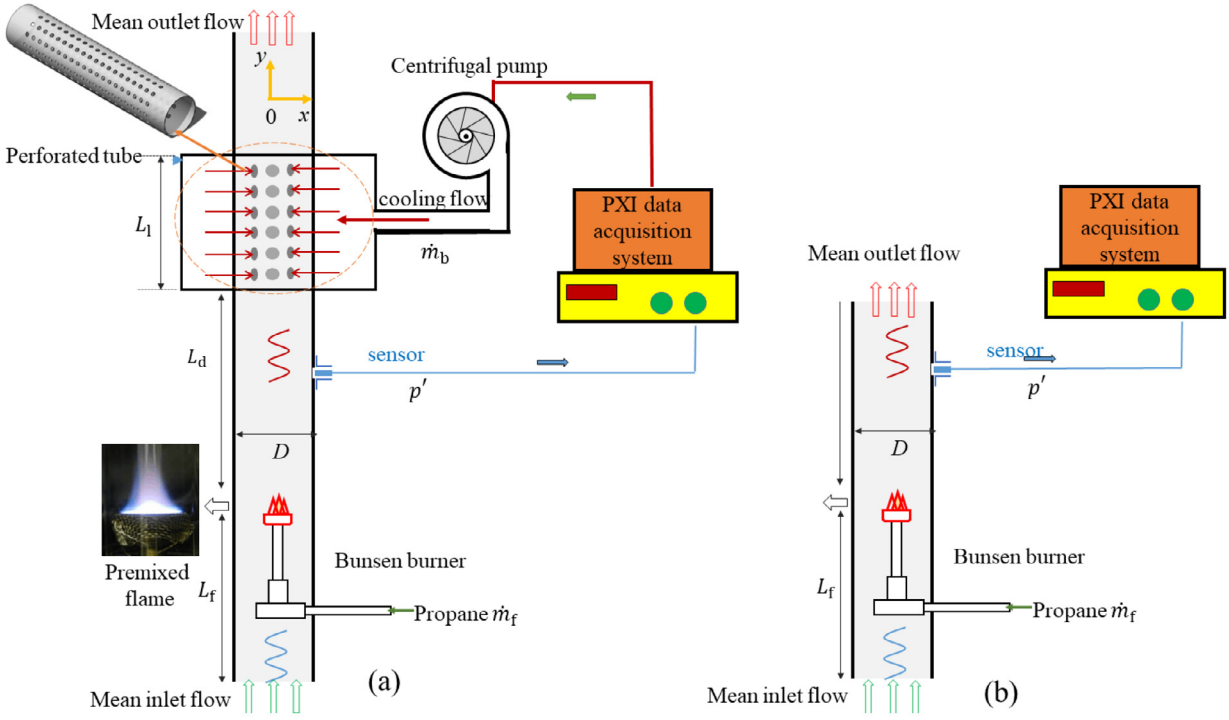

Fig. 6. (Color online) Schematic of (a) the experimental setup with a perforated pipe and a data processing unit implemented; (b) the conventional Rijke tube without the perforated pipe implemented.

Table 1
Geometric dimensions of the perforated pipe with circle-shaped orifices.

Parameters	Values
Perforated pipe length L_l	100.0 mm
Orifice diameter D_o	3.0 mm
Number of orifices per row	14
Ambient pressure p_0	1.01325×10^5 Pa
Porosity η_o	5.1%
Air density ρ_0	1.2 kg/m^3
Orifice thickness h_o	5.0 mm
Number of rows	8
Ambient temperature T_0	297 K
Pipe inner diameter D	45 mm

tion. In this case, the setup is converted into the classical Rijke-type combustor as shown in Fig. 6b. The obtained experimental results are summarized in Fig. 9. It can be seen that as the lined section is suddenly removed at $t = 22$ s, the limit cycle oscillations becomes large-amplitude beating ones. Close observation is made by plotting the phase diagrams at $5 \leqslant t \leqslant 6$ s and $25 \leqslant t \leqslant 26$ s, as shown in Fig. 9b and c. In the presence of the perforated pipe backed by the cavity, thermo-acoustic oscillations are present and a circle-shaped phase diagram is obtained. It represents the typical sinusoid waveform signal. It indicates that there is a dominant mode. However, as the perforated pipe section is removed, a circle-belt shaped phase diagram is observed. This reveals that there are multiple dominant modes. It is worth noting that the length of the Rijke tube does affect the combustion instability characteristics in terms of frequency and amplitude [55,56]. This is due to the mode-shape present along the combustor, as the liner is attached or not. When there is no lined section, the total length of the Rijke tube is shorter. Since the tube length (both ends are pressure nodes) is corresponding to half of the wavelength and thus the frequency of the dominant mode is higher. However, when the lined section is attached to the Rijke tube, the total length is increased. And the frequency of the dominant mode is decreased.

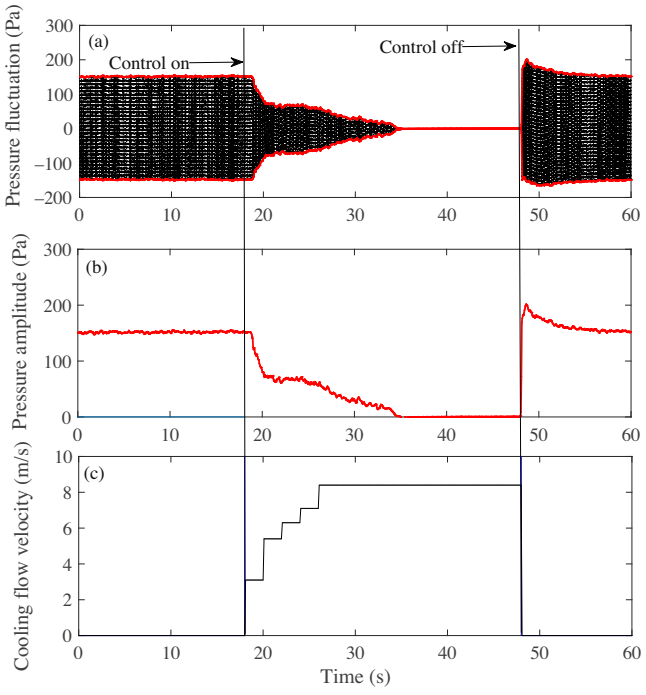

Fig. 7. (Color online) Time trace of the measured pressure fluctuation (a) pressure amplitude (b) controllable bias flow rate (c) in the lined Rijke-type combustion system.

To gain insights on the beating oscillations, the frequency spectrum and probability density function (PDF) of the measured pressure fluctuations are obtained. This is shown in Fig. 10. It is clear that in the presence of beating oscillations, there is a very low-frequency mode at $\omega_{rmf} = 1.4$ Hz in addition to the thermo-acoustic mode at $\omega_1 \approx 245$ Hz. Furthermore, there are harmonics

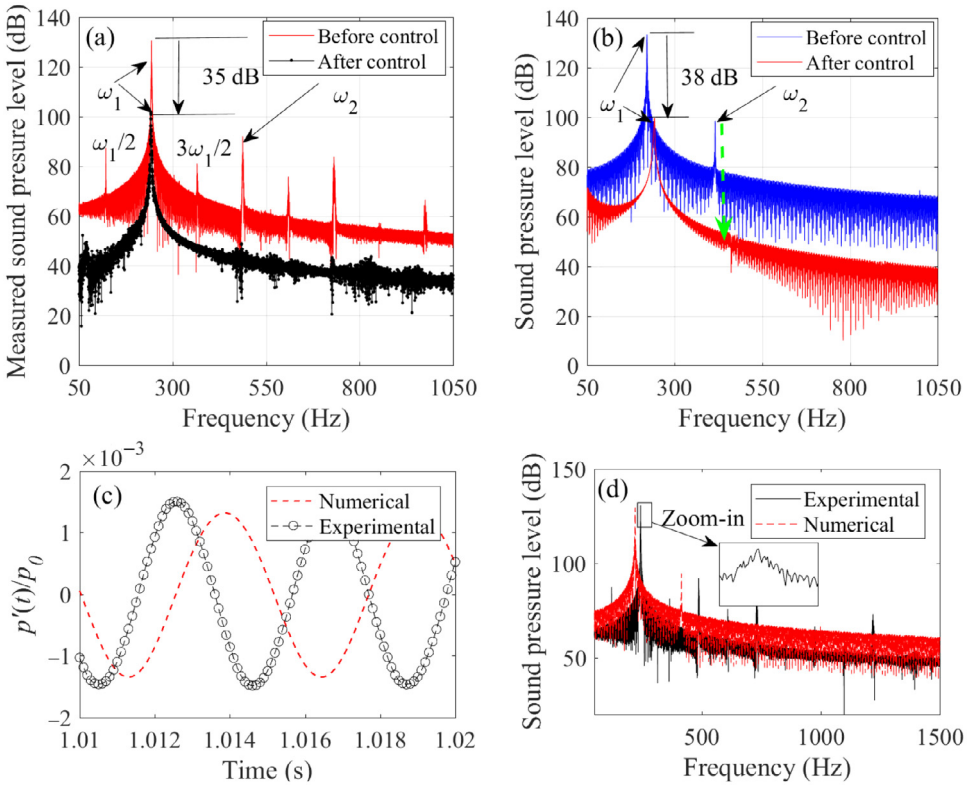

Fig. 8. (Color online) Frequency spectrum of the experimental (a) and predicted (b) pressure fluctuation from the lined Rijke-type combustion system before and after control (i.e. implementing cooling flow), (c) comparison between predicted pressure fluctuations and measured ones in time domain, (d) comparison of the frequency spectrum of the predicted and measured pressure fluctuations.

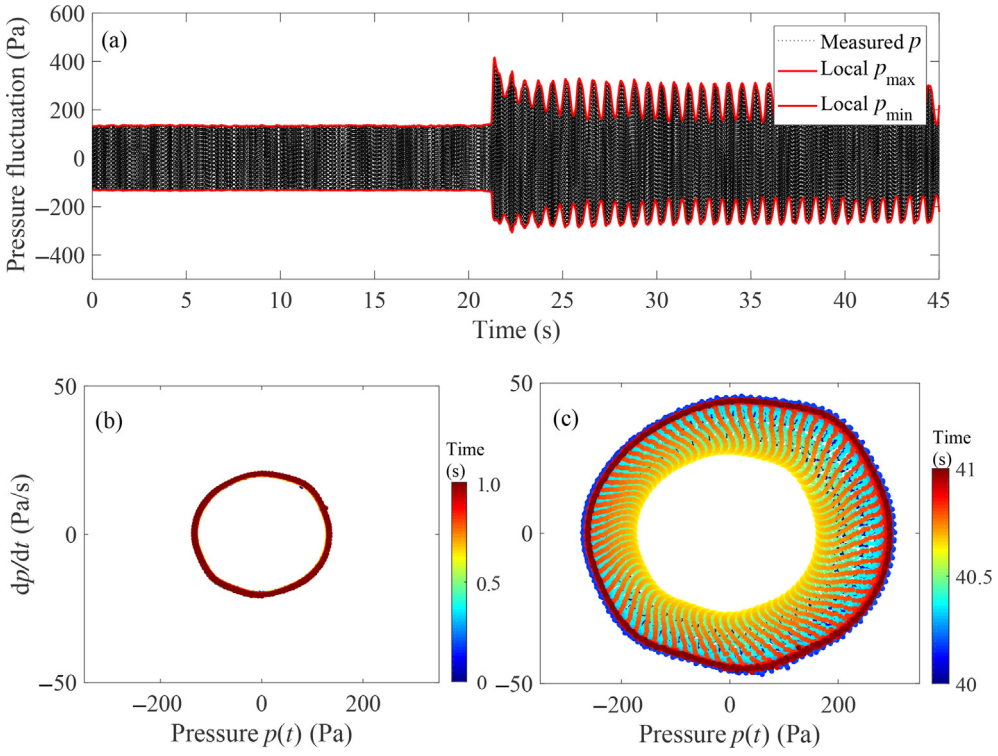

Fig. 9. (Color online) Time evolution of the combustion-excited pressure oscillations before and after removing the lined section.

of the low-frequency mode at ω_{rmf} and the thermo-acoustic mode at ω_1. It reveals that the combustion system is nonlinear, as shown in Fig. 10a.

The statistical characteristics [5] of the measured oscillations in the presence or absence of the perforated pipe section are illustrated by the probability density function (PDF) of $p'(t)$ in Fig. 10b. It can be seen that the pressure distribution peaks at $\|p'(t)\| \approx 152$ Pa and has a U-shaped distribution about its mean, as the perforated pipe is applied. Such U-shaped PDF represents a typical sinusoid waveform. However, the U-shaped distribution is quite different from the M-shaped distribution. The M-shaped distribution represents a superposition of two or more sinusoid waveforms with comparable amplitudes but different frequencies. The pressure distribution becomes more uniformed and broad.

To identify the generation mechanism of such low-frequency mode, flame motion is experimentally recorded. Fig. 11 illustrates the periodic motion of the flame at 4 different time instants, which are captured by a high speed camera. It can be seen that the flame is undergoing a "pulsating" motion with a period of $T_{\mathrm{rmf}} = 2\pi/\omega_{\mathrm{rmf}} \approx 0.71$ s. For illustration and demonstration, a recorded video of the flame motion and combustion-driven noises is supplied as a Supplementary material. Both loud combustion noise and flame "pulsating" motion are clearly observed. It reveals that in the absence of the perforated pipe, flame pulsating oscillations are superimposed on the combustion-excited thermo-acoustic oscillations. These 2 types of oscillations are associated with dramatically different time scales. One is associated with a period of $1/245 \approx 0.0041$ s and the other is $1/1.4 \approx 0.71$ s. These periods are fundamentally different. The large-period pulsating oscillations can be attributed to the thermal-diffusive effects, whereas shorter-period combustion-excited oscillations [48–50] correspond to acoustic resonances of the Rijke-type combustor. Further study confirms that introducing the acoustic damping/loss [51] to a combustor by implementing the perforated pipe, even in the absence of a cooling flow, can attenuate the thermal-diffusive instability. Such thermal-diffusive instability is conventionally believed to be strongly coupled with periodic thermo-acoustic oscillations. These periodic oscillations may promote flame pulsating motions by increasing flame heat loss, as discussed by Weng et al. [10].

The acoustical energy consists of both potential and kinematic energy [53]. Thus, it is reasonable to assume that the acoustical energy $\sum \mathcal{E}_n$ is proportional to the potential energy. Mathematically, $\sum \mathcal{E}_n \approx \frac{\pi D^2}{4} \frac{|p'|^2}{\gamma p_0}$. The measured acoustic potential energy flux from the lined Rijke (LR) tube and the classical Rijke (CR) tube without the perforated pipe are compared, as shown in Fig. 12a. It can be seen that the lined Rijke tube is associated with enhanced acoustic losses (resulting from the perforated pipe) in comparison with that in the classical Rijke tube. However, no thermal-diffusive instability is observed. The relative change of the acoustic potential energy flux with and without the perforated pipe is shown in Fig. 12b. It can be seen that the potential energy flux is changed between 30% and 83% and so the acoustic losses introduced by implementing the perforated pipe. This suggests that decreased acoustic losses trigger the thermal-diffusive instability.

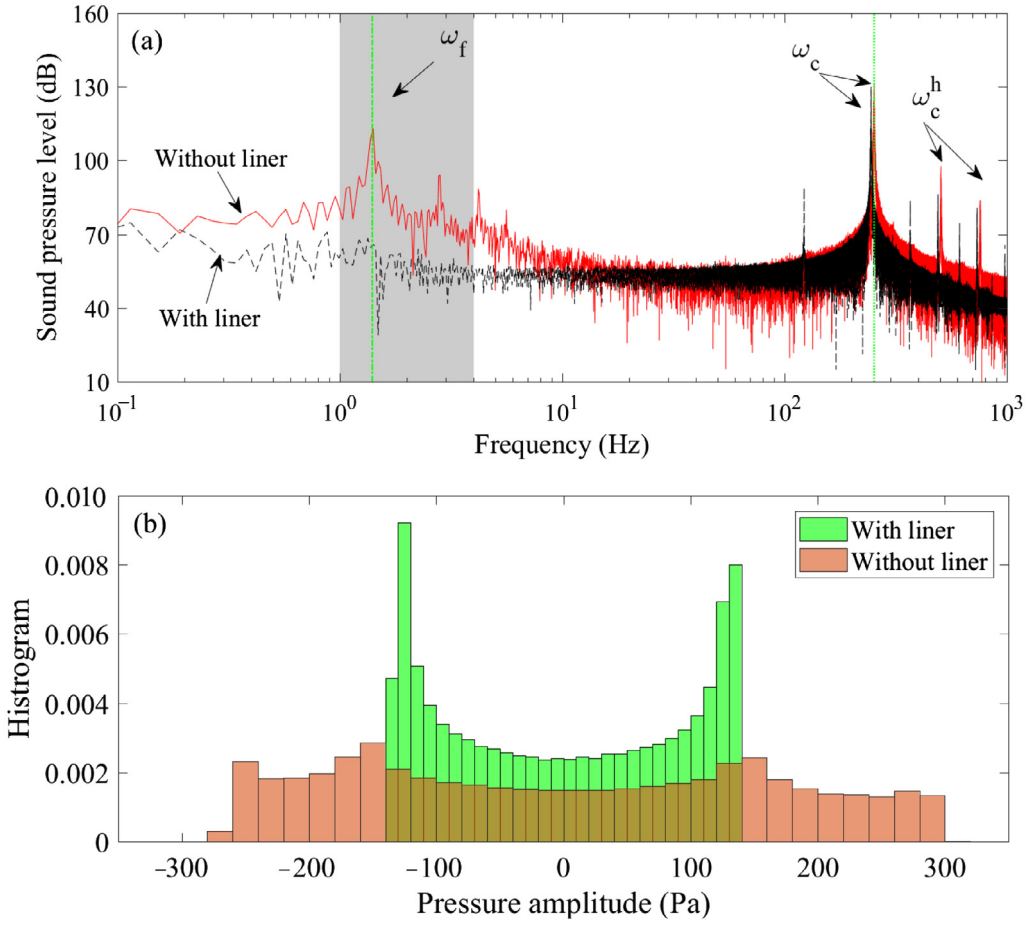

Fig. 10. (Color online) Comparison of (a) the frequency spectrum and (b) probability density function (PDF) (b) of the measured pressure oscillations before and after the lined section being removed.

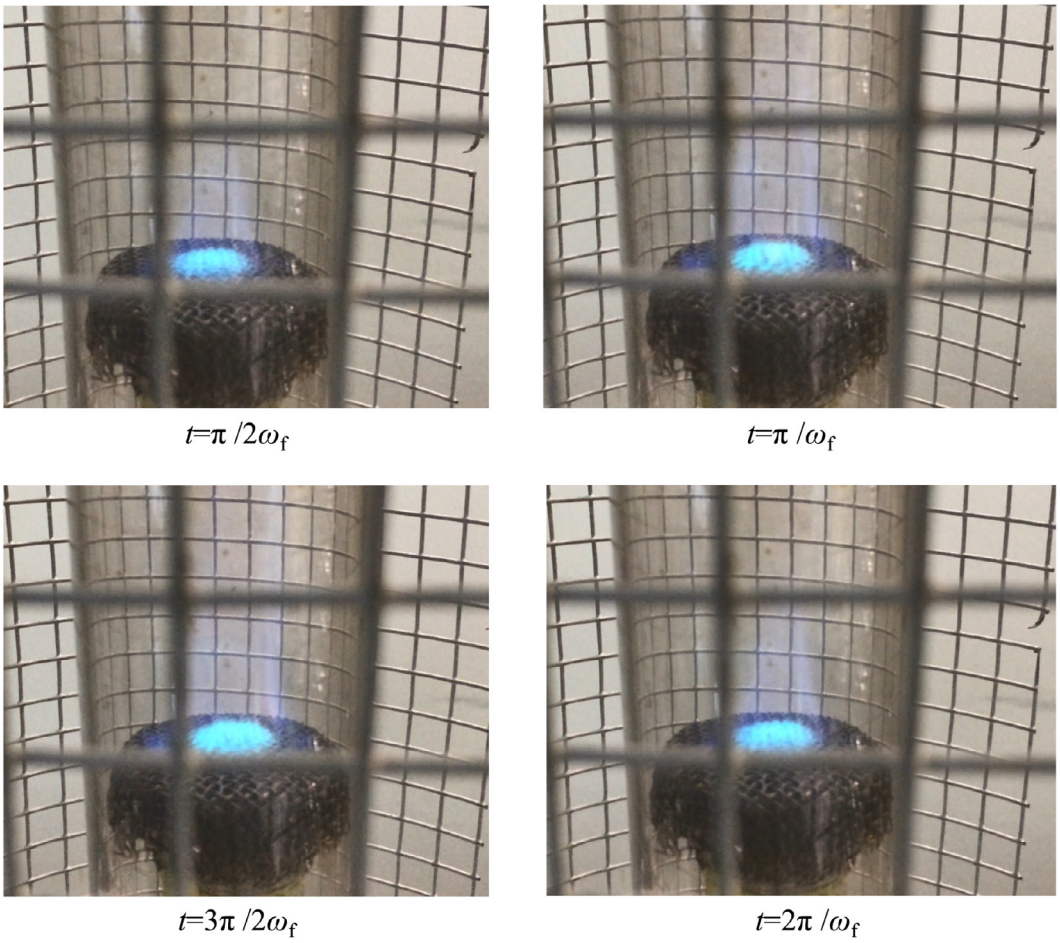

Fig. 11. (Color online) Flame motion images over a period of $\omega_{rmf}/2\pi \approx 0.71$ s (see attached Video).

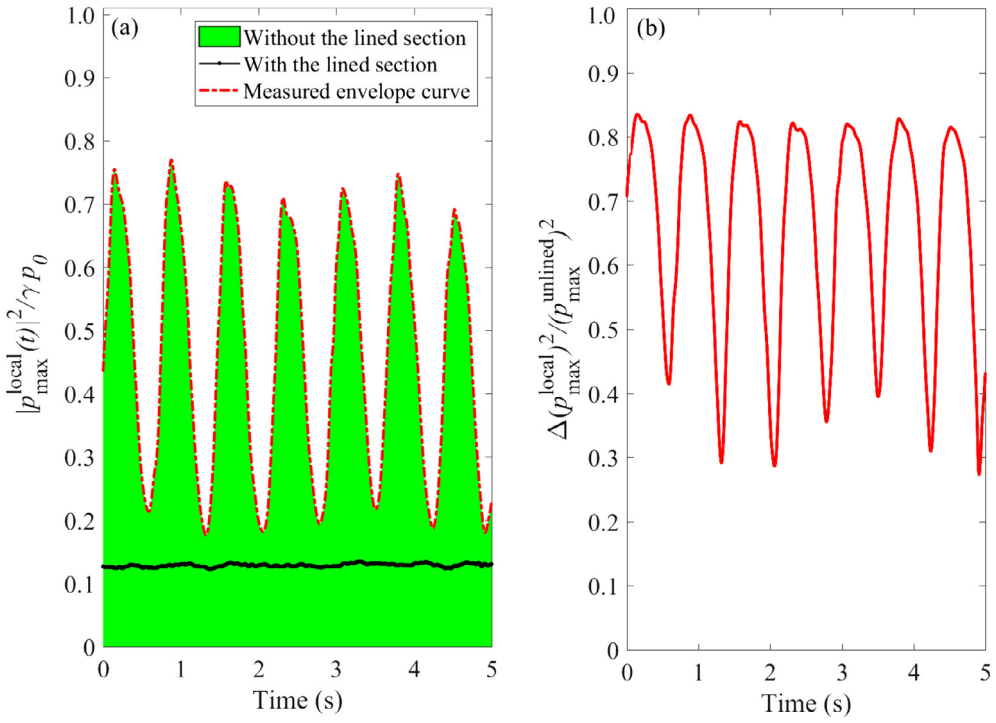

Fig. 12. (Color online) Comparison between the lined Rijke tube and the classical Rijke tube without the perforated liner (a) the measured acoustic losses, (b) the acoustic potential energy flux change.

5. Conclusions

To mitigate combustion instabilities, active open-loop control of a low-porosity perforated pipe with a cooling flow is conducted on a Rijke-type thermoacoustic combustor. For this, both numerical and experimental studies are conducted. A 2D numerical model of a lined Rijke-type combustor is developed first. Numerical results reveal that the model can not only successfully produce limit cycle combustion-excited oscillations but be used to evaluate the performance of the control strategy. As the cooling flow rate through the perforated pipe is actively tuned, combustion-excited oscillations can be completely attenuated. A wavy flame front in the presence of thermo-acoustic oscillations is changed to be a more smooth conical shape, when the oscillations are attenuated. In addition, the vorticity-induced acoustic damping contribution of the perforated pipe is not uniformly distributed along the axial direction of the combustor. The downstream of the perforated pipe contributes more to the attenuation performance of the control strategy. This may be due to the acoustics mode shape. Further downstream means more closer to the pressure node and larger pressure difference across the perforated pipe.

To evaluate the performance of the control approach in practice and to confirm the numerical findings, a lined Rijke-type combustor is designed and tested. A low porosity perforated pipe enclosed by a large cavity is attached to the classical Rijke-type combustor downstream of a premixed propane-fueled flame. The flame is anchored on top of a Bunsen burner, which is confined at the bottom part of the lined combustor. It is found that self-sustained combustion-oscillations occur in the absence of a cooling flow. To maximize the damping performance of the perforated pipe, the cooling flow rate is actively controlled, based on the measured pressure fluctuation. On implementing such active open-loop control strategy, the unstable combustor is successfully stabilized by reducing sound pressure level over 35 dB. Finally, the perforated pipe is found to be able to attenuate flame pulsating oscillations. Such flame oscillations are at extremely low frequency and result from the thermal-diffusive effect. The flame pulsating instability is quite different from the classical thermo-acoustic oscillations in terms of the generation mechanism and time scales. To achieve complete attenuation of combustion-driven oscillations, the mass flow ratio between the implemented cooling flow and the inlet flow is found to be approximately 330%. This critical ratio is much larger than the numerical prediction of approximately 205%. This could be due to the assumptions made in the modelled combustor. For example, the modelled perforated pipe is assumed to be adiabatic. In general, the present studies confirm that implementing perforated pipes with an appropriate amount of cooling flow could be an effective control strategy to stabilize gas turbine combustors and to attenuate combustion-driven tonable noise.

Conflict of interest

The authors declare that they have no conflict of interest.

Acknowledgments

This work was supported by the University of Canterbury, New Zealand with Grant No. 452STUPDZ, and National Research Foundation, Prime Minister's Office, Singapore, with Grant No. NRF2016NRF-NSFC001-102 and National Natural Science Foundation of China (11661141020).

Author contributions

D. Z. conducted the experimental measurements and contributed to the numerical computation with A. R.. D. Z. and E. G. analysed the numerical and experimental results. D. Z. conceived and initialized the project and wrote the paper with E. G.

Appendix A. Supplementary data

Supplementary data associated with this article can be found, in the online version, at https://doi.org/10.1016/j.scib.2019.05.004.

References

[1] Wang H, Zhang L, Yu G, et al. A looped heat-driven thermoacoustic refrigeration system with direct-coupling configuration for room temperature cooling. Sci Bull 2019;64:8–10.
[2] Luo E, Huang Y, Dai WA. high-performance thermoacoustic refrigerator operating in room-temperature range. Chin Sci Bull 2005;50:2662–4.
[3] Gullaud E, Nicoud F. On the effect of perforated plates on the acoustics of annular combustors. AIAA J 2012;50:2629–42.
[4] Noiray N, Schuermans B. Theorectical and experimental investigations on damper performance for suppression of thermoacoustic oscillations. J Sound Vib 2012;331:2753–63.
[5] Lieuwen TC. Experimental investigation of limit-cycle oscillations in an unstable gas turbine combustor. J Propul Power 2002;18:61–7.
[6] Pan H, Bi Q, Liu Z, et al. Experimental investigation on thermo-acoustic instability and heat transfer of supercritical endothermic hydrocarbon fuel in a mini tube. Exp Thermal Fluid Sci 2018;97:109–18.
[7] Allouis C, Amoresano A, Langella G, et al. Characterization of gas turbine burner instabilities by wavelet analysis of infrared images. Exp Thermal Fluid Sci 2016;73:94–100.
[8] Chatterjee P, Vandsburger U, Saunders WR, et al. On the spectral characteristics of a self-excited Rijke tube combustor-numerical simulation and experimental measurements. J Sound Vib 2005;283:573–88.
[9] Margolis SB. Bifurction phenomena in burner-stabilized premixed flames. Combust Sci Technol 1980;22:143–69.
[10] Weng F, Li S, Zhong D, et al. Investigatin of self-sustained beating oscillations in a Rijke burner. Combust Flame 2016;166:181–91.
[11] Weng F, Zhu M, Jing L. Beat: a nonlinear thermoacoustic instability in Rijke burners. Int J Spray Combust Dyn 2014;6:247–66.
[12] Chrystie R, Chung SH. Response to acoustic forcing of lmainar coflow jet diffusion flames. Combust Sci Technol 2014;186:409–20.
[13] Yoon SH, Hu L, Fujita O. Experimental observation of pulsating instability under acoustic field in downward-propagating flames. Combust Flame 2018;188:1–4.
[14] Mejia D, Miguel-Bredion M, Ghani A, et al. Influence of flame-holder temperature on the acoustic transfer functions of a laminar flame. Combust Flame 2018;188:5–12.
[15] Kabiraj L, Sujith RI. Nonlinear self-excited thermoacoustic oscillations. J Fluid Mech 2012;713:376–97.
[16] Saurabh A, Paschereit CO. Dynamics of premixed swirl flames under the influence of transverse acoustic fluctuations. Combust Flame 2017;182:298–312.
[17] Li J, Xia Y, Morgans AS, et al. Numerical prediction of combustion instability limit cycle oscillations for a combustor with a long flame. Combust Flame 2017;185:28–43.
[18] Blumenthal RS, Subramanian P, Sujith RI, et al. Novel perspectives on the dynamics of premixed flames. Combust Flame 2013;160:1215–24.
[19] Hield PA, Brear MJ, Jin SH. Thermoacoustic limit cycles in a premixed laboratory combustor with open and choked exits. Combust Flame 2009;156:1683–97.
[20] Bigongiari A, Heckl MAA. Green's function approach to the rapid prediction of thermoacoustic instabilities in combustors. J Fluid Mech 2016;798:970–96.
[21] Zhang G, Wang X, Li L, et al. Control of thermoacoustic instability with a drum-like silencer. J Sound Vib 2017;406:253–76.
[22] Zhang Y, Huang L. Electroacoustic control of Rijke tube instability. J Sound Vib 2017;409:131–44.
[23] Zhao D, Ji C, Li S. Mitigation of premixed flame-sustained thermoacoustic oscillations using an electrical heater. Int J Heat Mass Transfer 2015;86:309–18.
[24] Cosic B, Bobusch BC, Moeck JP, et al. Open-loop control of combustion instabilities and the role of the flame response to two-frequency forcing. J Eng Gas Turbines Power 2012;134:061502.
[25] Uhm JH, Acharya S. Low-bandwidth open-loop control of combustion instability. Combust Flame 2005;142:348–63.
[26] Uhm JH, Acharya S. Role of low-bandwidth open-loop control of combustion instability using a high-momentum air jet-mechanic details. Combust Flame 2006;147:348–63.
[27] Richards GA, Thornton JD, Robey EH, et al. Open-loop active control of combustion dynamics on a gas turbine engine. J Eng Gas Turbines Power 2007;129:38–48.
[28] Richards GA, Straub DL, Robey EH. Passive control of combustion dynamics in stationary gas turbines. J Propul Power 2003;19:795–810.
[29] Li L, Guo Z, Zhang C, et al. A passive method to control combustion instabilities with perforated liner. Chin J Aeronaut 2010;23:623–30.

[30] Kelsall G, Troger C. Prediction and control of combustion instabilties in industrial gas turbines. Appl Thermal Eng 2004;24:1571–82.
[31] Steele RC, Cowell LH, Cannon SM, et al. Passive control of combustion instability in lean premixed combustors. J Eng Gas Turbines Power 2000;122:412–9.
[32] Gotoda H, Shinoda Y, Kobayashi M, et al. Detection and control of combustion instability based on the concept of dynamical system theory. Phys Rev E 2014;89:022910.
[33] Hathout JP, Fleifil M, Annaswamy AM, et al. Combustion instability active control using periodic fuel injection. J Propul Power 2002;18:390–9.
[34] Olgac NA. study of Helmholtz resonators to stabilize thermoacoustically driven pressure oscillations. J Acoust Soc Am 2016;139:1962–73.
[35] Rupp J, Carrotte J, Macquisten MA. The use of perforated damping liners in aero gas turbine combustion systems. J Eng Gas Turbines Power 2011;134:495–506.
[36] Zhao D, Morgans AS, Dowling AP. Tuned passive control of acoustic damping of perforated liners. AIAA J 2011;49:725–34.
[37] Williams LJ, Meadows J, Agrawal AK. Passive control of thermoacoustic instabilities in swirl-stablized combustion at elevated pressures. Int J Spray Combust Dyn 2016;8:173–82.
[38] Zhang Q, Bodony DJ. Numerical investigation and modelling of acoustically excited flow through a circular orifice backed by a hexagonal cavity. J Fluid Mech 2012;693:367–401.
[39] Lawn C. Calculation of acoustic absorption in ducts with perforated liners. Appl Acoust 2015;89:211–21.
[40] Tam CKW, Kurbatskii KA, Ahuja KK, et al. A numerical and experimental investigation of the dissipation mechanisms of resonant acoustic liners. J Sound Vib 2001;245:545–57.
[41] Jing XD, Sun XF. Effect of plate thickness on impedance of perforated plates with bias flow. AIAA J 2000;38:1573–8.
[42] Eldredge JD, Dowling AP. The absorption of axial acoustic waves by a perforated liner with bias flow. J Fluid Mech 2003;485:307–35.
[43] Motheau E, Nicoud F, Poinsot F. Mixed acoustic-entropy combustion instabilities in gas turbines. J Fluid Mech 2014;749:542–76.
[44] Cook DJ, Pitsch H, Peters N. Numerical simulation of combustion instabilities in a lean premixed combustor with finite rate chemistry. ASME Turbo Expo 2003;2:429–38.
[45] Tran N, Ducruix S, Schuller T. Damping combustion instabilities with perforates at the premixed inlet of a swirl burner. Sci China Press Proc Combust Inst 2009;32:2917–24.
[46] Howe MS. The influence of tangential mean flow on the Rayleigh conductivity of an aperature. Proc R Soc Lond A 1996;452:2303–14.
[47] Versteeg HK, Malalasekera W. An introduction to computational fluid dynamics: the finite volume method. 2nd ed. Pearson Education Ltd; 2007. pp. 213–314.
[48] Merk M, Janensch S, Silva C, et al. Simultaneous identification of transfer functions and combustion noise of a turbulent flame. J Sound Vib 2018;422:432–52.
[49] Gupta V, Saurabh A, Paschereit CO, et al. Numerical results on noise-induced dynamics in the subthreshold regime for thermoacoustic systems. J Sound Vib 2017;390:55–66.
[50] Webster S, Hardi J, Oschwald M. Measurement of acoustic dissipation in an experimental combustor under representative conditions. J Sound Vib 2017;390:39–54.
[51] Hoeijmakers M, Kornilov V, Arteaga IL, et al. Flame dominated thermoacoustic instabilities in a system with high acoustic losses. Combust Flame 2016;169:209–15.
[52] McManus KR, Poinsot T, Candel SM. A reivew of active control of combustion instabilities. Prog Energy Combust Sci 1993;19:1–29.
[53] Carmicino C, Di Martino GD. Analytical modeling of the one-dimensional acoustic field in hybrid rocket combustion chamber. J Sound Vib 2018;437:180–97.
[54] Mensah GA, Magri L, Silva CF, et al. Exceptional points in the thermoacoustic spectrum. J Sound Vib 2018;433:124–8.
[55] Carvalho Jr JA, Ferreira MA, Bressan C, et al. Definition of heater location to drive maximum amplitude acoustic oscillations in a Rijke tube. Combust Flame 1989;76:17–27.
[56] Zhao D, Chow ZH. Thermoacoustic instability of a laminar premixed flame in Rijke tube with a hydrodynamic region. J Sound Vib 2013;332:3419–37.

Dan Zhao obtained his Ph.D. degree from the University of Cambridge in 2009. He is the director of Master Engineering Studies, at University of Canterbury, New Zealand. His research interests include thermoacoustics, aeroacoustics, energy harvesting, noise control, wind power, oxy-fuel/cavity combustion, micro-combustion, propulsion and aerodynamics.